ISSN 1063-7788, Physics of Atomic Nuclei, 2024, Vol. 87, No. 9, pp. 1355–1362. © Pleiades Publishing, Ltd., 2024.
Russian Text © The Author(s), 2025, published in Yadernaya Fizika i Inzhiniring, 2025, Vol. 16, No. 3.

CHARGED PARTICLE ACCELERATORS FOR NUCLEAR TECHNOLOGIES

Transition Energy Crossing in Harmonic RF at Proton Synchrotron U-70

S. D. Kolokolchikov[a,b,*], Yu. V. Senichev[a,b], and V. A. Kalinin[c]

[a] *Institute of Nuclear Research, Russian Academy of Sciences, Moscow, 117312 Russia*

[b] *Moscow Institute of Physics and Technology (National Research University), Dolgoprudny, Moscow oblast, 141701 Russia*

[c] *Logunov Institute of High Energy Physics, National Research Centre Kurchatov Institute, Protvino, Moscow oblast, 142281 Russia*

**e-mail: sergey.bell13@gmail.com*

Received May 5, 2024; revised June 24, 2024; accepted July 1, 2024

Abstract—Transition energy crossing at the U-70 proton synchrotron is studied. Motion stability is achieved through the method of transition energy jump at constant betatron tunes. The longitudinal motion is simulated with allowance for higher orders of the momentum compaction factor, along with various impedances and bunch intensities. Experimental data from an accelerator session are presented.

Keywords: transition energy, harmonic radio frequency resonator (RF), longitudinal dynamics, dispersion function modulation

DOI: 10.1134/S106377882410020X

INTRODUCTION

Transition energy crossing is an important problem for the proton beam in the NICA complex now under construction at the Joint Institute of Nuclear Research in Dubna. To study this problem, the dynamics of longitudinal motion in the vicinity of the transition energy of U-70 is investigated at the Institute of High Energy Physics in Protvino.

Increasing the rate of transition energy crossing reduces the influence of factors disturbing the phase motion. Transition energy jump method is used in many facilities at CERN [1] and BNL [2], and is done in the U-70. The transition energy is shifted by distorting the dispersion function with thin quadrupole lenses [3].

The results of this study will help highlight the potential consequences of transition energy crossing and determine the important parameters that affect the dynamics of phase motion.

EQUATIONS OF LONGITUDINAL MOTION

The equations of longitudinal motion describe the evolution of a particle in phase space relative to the reference [4]:

$$\begin{aligned}\frac{d\tau}{dt} &= \frac{\eta h}{\beta^2 E_0} E,\\ \frac{d\Delta E}{dt} &= \frac{Ze}{A}\frac{\omega_0}{2\pi} V\left[\sin(\phi_s - h\omega_0\tau) - \sin\phi_s\right],\end{aligned} \tag{1}$$

where τ is a temporary deviation of the considered particle from the reference particle; β is the relative velocity; $\omega_0 = 2\pi/T_0$ is the angular velocity and corresponding period of revolution; h is the harmonic number; V is the RF amplitude; ϕ_s is the equilibrium particle phase; and the slip-factor is $\eta(\delta) = \eta_0 + \eta_1\delta + \cdots$,

$$\eta_0 = \alpha_0 - \frac{1}{\gamma_0^2},\ \eta_1 = \frac{3\beta_0^2}{2\gamma_0^2} + \alpha_1 - \alpha_0\eta_0.$$

If the beam energy in Eq. (1) approaches the transition value $\gamma \to \gamma_{tr}$, $\eta = \eta_0 \to 0$ and the right-hand side of the equation vanishes. Stability must be ensured at transition energy crossing.

ADIABATICITY AND NONLINEARITY

Away from the transition energy, the frequency of the synchrotron oscillations varies slightly over time, and the motion is adiabatic. Near the transition energy, the condition of the adiabaticity of synchrotron motion is violated. The characteristic period of adiabaticity can be estimated by comparing the synchrotron frequency to the rate of the separatrix change (Fig. 1a) [5]:

$$\tau_{\text{ad}} = \left(\frac{\pi\beta^2 mc^2\gamma_{\text{tr}}^4}{\dot{\gamma}\omega_0^2 heV\left|\cos\phi_s\right|}\right)^{1/3}, \tag{2}$$

where γ_{tr} is the Lorentz factor corresponding to the transition energy and $\dot{\gamma}$ is the rate of change in energy.

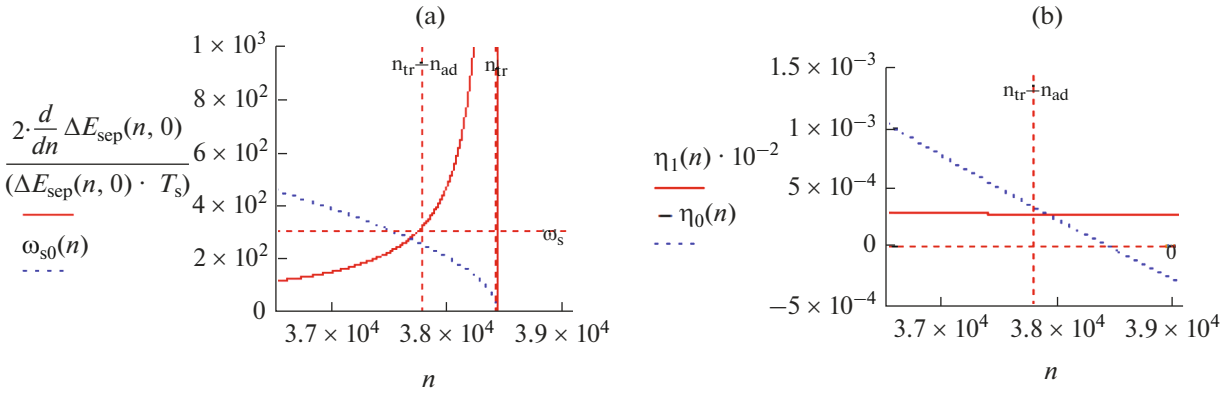

Fig. 1. (a) Classic synchrotron frequency and rate of change of the separatrix envelope in the vicinity of the transition energy as a function of the turn number; (b) first- and second-order change in slip-factor η_0, $\eta_1\delta$ in the vicinity of the transition energy as a function of the turn number.

The nonlinearity of longitudinal motion is seen when the characteristic period is comparable to (Fig. 1b)

$$\tau_{nl} = \frac{\eta_1\hat{\delta}}{\frac{2\dot{\gamma}}{\gamma_{tr}^3}} = \gamma_{tr}\frac{\frac{3}{2}\beta^2 + \gamma_{tr}^2\alpha_1}{2\dot{\gamma}}, \quad (3)$$

where $\hat{\delta} \approx 10^{-2}$–$10^{-3}$ is the absolute value of the maximum deviation of the momentum near the transition energy and α_1 is the second order of the momentum compaction factor. It was found in [6] that $\alpha_1 \simeq 0.01$ for the regular FODO structure of the U-70 with natural chromaticity compensated for. Equation (1) also yields the condition for the stability of synchrotron oscillations,

$$\eta_0 \cos\phi_s < 0. \quad (4)$$

Table 1. Main parameters of the RF and U-70 ring

Length L, m	1483.699
Momentum compaction factor α_0	0.011120
Momentum compaction factor α_1	0.01
Transition energy, GeV	7.957
Lorentz factor γ_{tr}	7.48
Maximum intensity during the session, ppp (particles per period)	4×10^{12}
Accelerating phase $\sin(\phi_s)$	1/2
Adiabatic time τ_{ad}, ms	3.218
Nonlinear time τ_{nl}, ms	2.646
Harmonic number	30
Accelerating station amplitude, kV	10
Number of accelerating stations	40
Rate of acceleration $\dot{\gamma}$, s^{-1}	42.7

It is apparent that the phase of the RF accelerating field must also be shifted after transition energy crossing to obtain longitudinal matching. The estimates for U-70 presented in Table 1 show that adiabatic period (2) can be comparable to nonlinearity period (3): $\tau_{ad} \sim \tau_{nl}$. The longitudinal length of the beam shrinks as the energy approaches the transition value, and the momentum spread grows. Figure 2 shows results from modeling the transition energy crossing when accelerating particles from 7 to 13 GeV for $\eta = \eta_0$ and $\eta = \eta_0 + \eta_1\delta$ in different BLonD models [7]. The effect of the second-order slip-factor raises the longitudinal emittance.

EFFECT OF INDUCTIVE IMPEDANCE

The longitudinal dynamics is also affected by the accelerator elements. Impedance describes the interaction between the beam and elements of the accelerator's structure. Longitudinal impedance $Z_{\|}(\omega)$ is especially important when studying the dynamics of transition energy crossing. Analytical calculations of the ring's total impedance are complicated, and we are limited here to its inductive component $Z_n/n = \pm i\times\text{const}$. Negative inductance corresponds to the impedance of the smooth chamber; positive inductance, to the longitudinal coupling impedance of pickup electrodes, kicker magnets, and bellows [3].

In our U-70 session, the intensity of a pulse was on the order of $N_{tot} = 4\times10^{12}$ ppp (particles per period). In a bunch, it was on the order of $N_{beam} = 4\times10^{11}$ ppb (particles per beam). Modeling the longitudinal dynamics with energies changing from 7 to 9 GeV showed that the beam remained stable at low intensity $N_{beam} = 4\times10^{11}$ for both negative and positive values of the considered impedance. A strong change in the symmetry of the phase volume and an increase in the

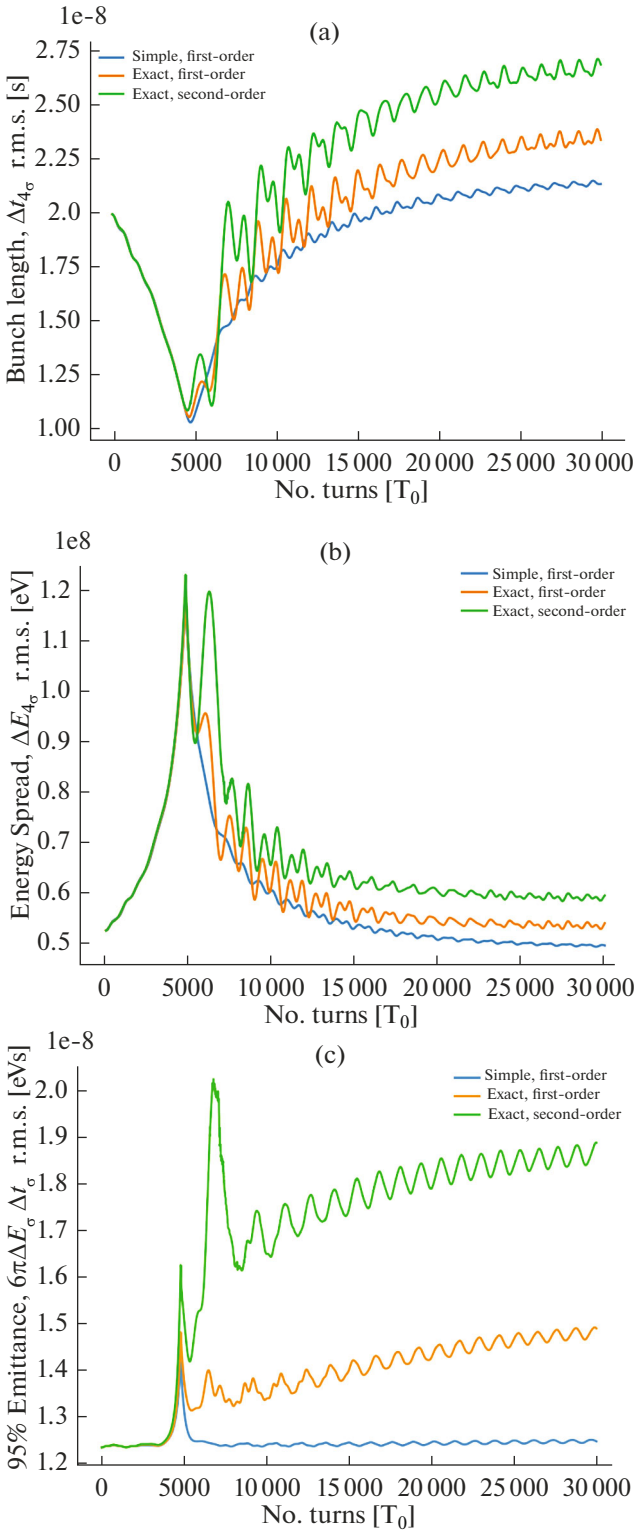

Fig. 2. Dependence of (a) the bunch length, (b) the energy spread inside the bunch, and (c) the longitudinal emittance on the turn number in the vicinity of the transition energy upon changing it from 7 to 13 GeV for three models without a jump, and allowing for impedance. The blue curve reflects only the first order $\eta = \eta_0$ for a simple solver; orange, only the $\eta = \eta_0$ of an exact solver; and green, only $\eta = \eta_0 + \eta_1\delta$.

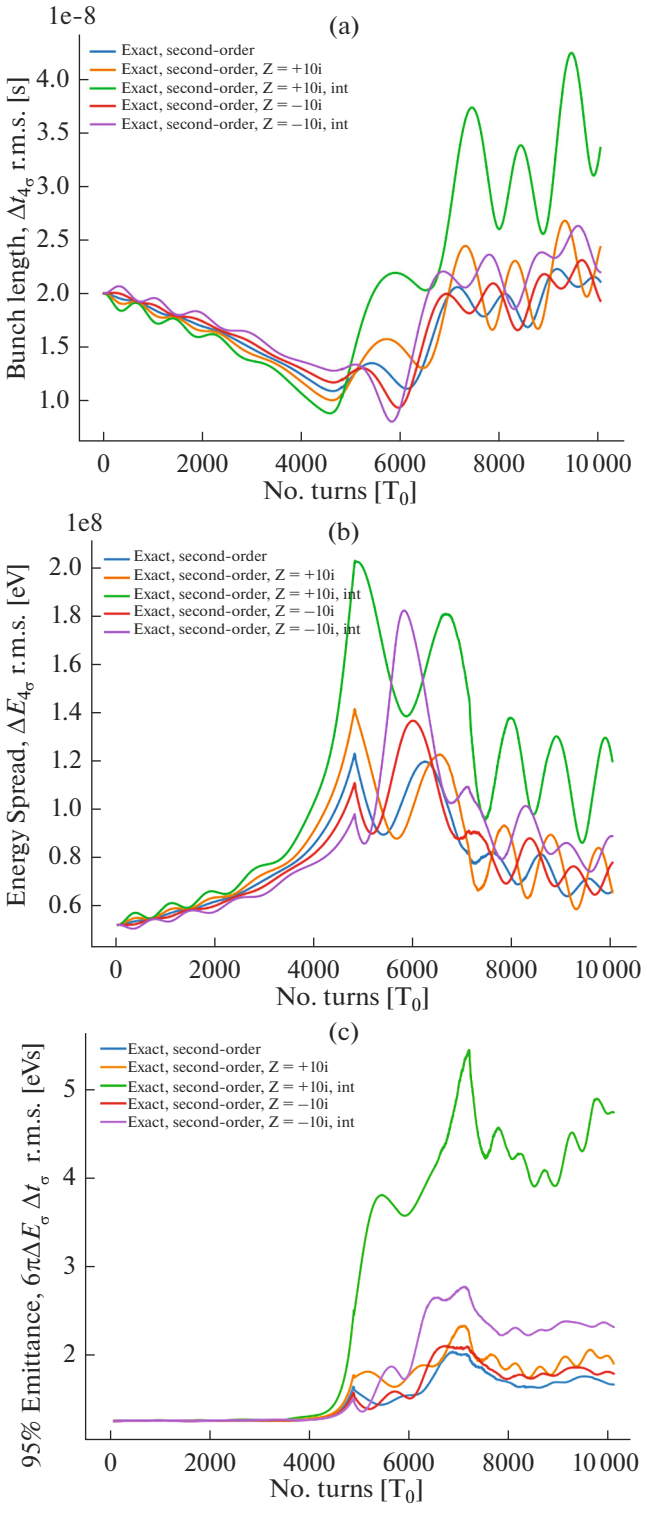

Fig. 3. Dependene of (a) the bunch length, (b) the energy spread inside the bunch, and (c) the longitudinal emittance on the turn number in the vicinity of the transition energy upon changing the energy from 7 to 9 GeV without a jump, allowing for different types of impedance and intensities.

Table 2. The results of numerical simulation of transition energy crossing, taking into account the influence of different impedances for different intensities

Modeling parameters	95% phase volume	Preservation of the beam (9 GeV)	Features
$\alpha_1 = 0$, simple Without impedance	1.23	100%	Simple model Emittance does not increase
$\alpha_1 = 0$, exact Without impedance	1.4	99.65%	Exact model, no MCF nonlinearity, influence of nonadiabaticity, increased emittance
$\alpha_1 = 0.01$, exact Without impedance	1.8	99.65%	Effect of MCF nonlinearity Emittance grows by 1.5 times
$\alpha_1 = 0.01$, exact $Z_n/n = -i10$ 4×10^{11} ppb	1.8	99.65%	Bunch length shrinks after γ_{tr}, focusing after γ_{tr} Increased emittance
$\alpha_1 = 0.01$, exact $Z_n/n = +i10$ 4×10^{11} ppb	1.9	99.60%	Bunch length shrinks after γ_{tr}, wiggling after γ_{tr} Increased emittance
$\alpha_1 = 0.01$, exact $Z_n/n = -i10$ 1×10^{12} ppb	2.3	99.60%	Strong reduction in bunch length before γ_{tr}, increased emittance
$\alpha_1 = 0.01$, exact $Z_n/n = +i10$ 1×10^{12} ppb	4.1	98.60%	Enhanced amplitude of quadrupole oscillations; strong increase in emittance

longitudinal emittance were observed for high intensities $N_{beam} = 1\times10^{12}$ (Fig. 3, Table 2). According to the experimental data, the initial value of the bunch length was $\tau_L = 4t_\sigma \simeq 20$ ns for $E_0 = 7$ GeV.

For a Gaussian distribution, $\Delta E_0 = 4E_\sigma = 52.7$ MeV, $\varepsilon_{095\%} = 1.23$ eV s.

TRANSITION ENERGY JUMP

To maintain stability of longitudinal motion, the longitudinal emittance should not grow during transition energy crossing. The U-70 therefore uses transition energy jump [8]. The rate of transition energy grows, while acceleration rate does not. This is achieved by altering the parameters of the accelerator to change α_0. The momentum compaction factor is generally defined as the integral

$$\alpha = \frac{1}{C}\int_0^C \frac{D(s)}{\rho(s)}ds, \qquad (5)$$

where $D(s)$ is the dispersion function and $\rho(s)$ is the orbital curvature. The momentum compaction factor can be changed by modulating the dispersion function, since $\rho(s)$ does not changed.

Such modulation in the U-70 synchrotron is done by quadrupoles in the 2nd and 8th blocks of each

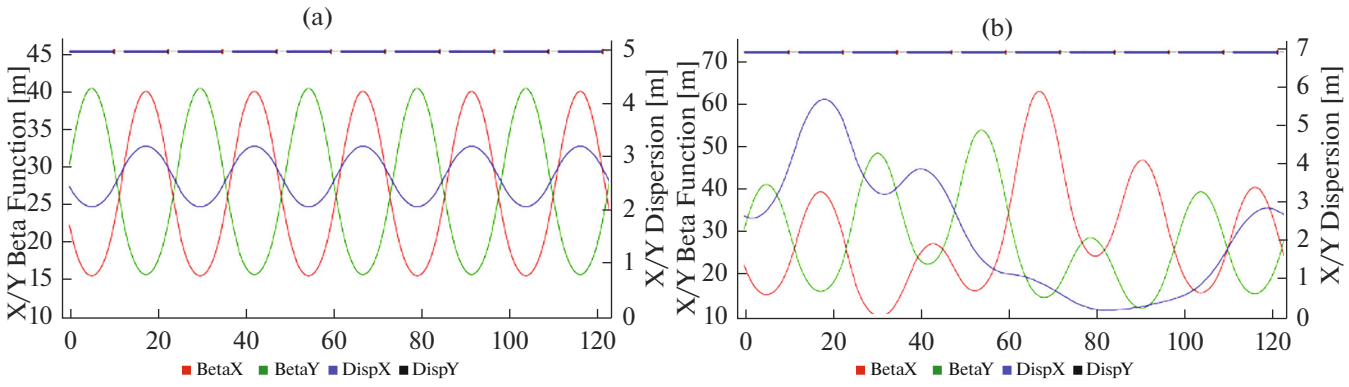

Fig. 4. Twiss parameters β_x, β_y, D_x for the U-70 superperiod: (a) regular structure; (b) structure with modulated dispersion.

Table 3. Changing the operating point during transition energy jump procedure at U-70

Time after injection, ms	Operating point	Relative to the jump
290	9.921×9.842	before the procedure
295	9.917×9.808	start of the procedure
310	9.849×9.787	middle of the procedure
326	9.780×9.771	moment of the jump
330	9.902×9.809	after

superperiod [9]. Figure 4 shows the Twiss parameters for one superperiod consisting of 10 magnetic blocks with a combined function for both the regular U-70 structure and a structure with a distorted dispersion function [10]. The quadrupoles positioned at every half period have opposite polarities. There is no shift in the operating point with such dispersion modulation. Table 3 gives the values of the operating point during transition energy increasing and jump. The transition energy is thus raised at the leading edge by $\Delta\gamma_{tr} = 0.9$ for 36 ms, and the jump itself takes 1ms at the trailing edge. A schematic diagram of the procedure is shown in Fig. 5, along with the corresponding first-order change in the slip-factor. The jump procedure at our U-70 session is described in Fig. 6a; the longitudinal linear density of the bunch relative to the RF phase at the moment of the jump is displayed in Fig. 6b.

The data from modeling the longitudinal motion correspond to the change in the bunch length during the acceleration cycle at our U-70 session (Fig. 7).

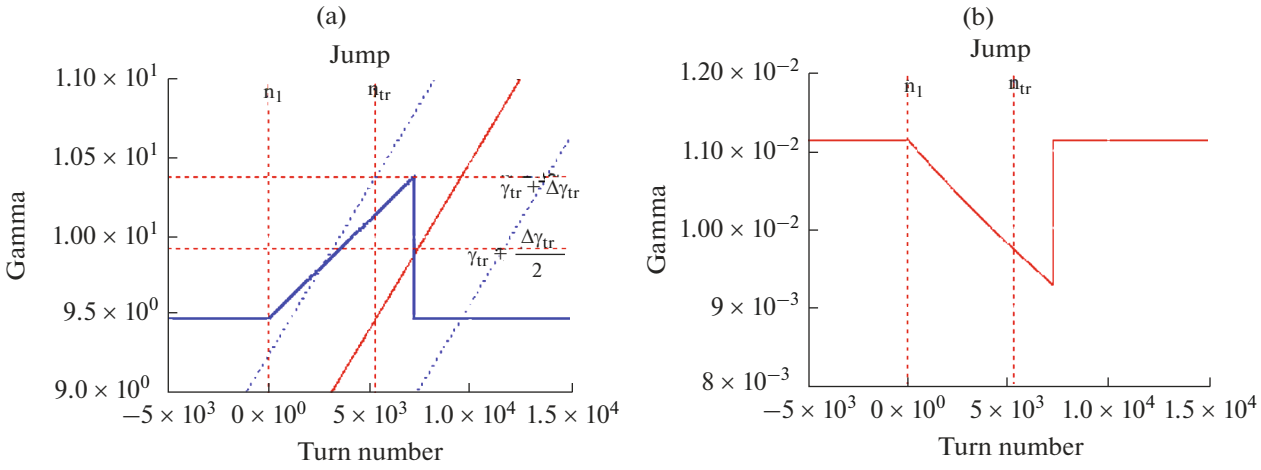

Fig. 5. (a) Increase of transition energy during the jump procedure; (b) corresponding change in the first order of slip-factor η_0.

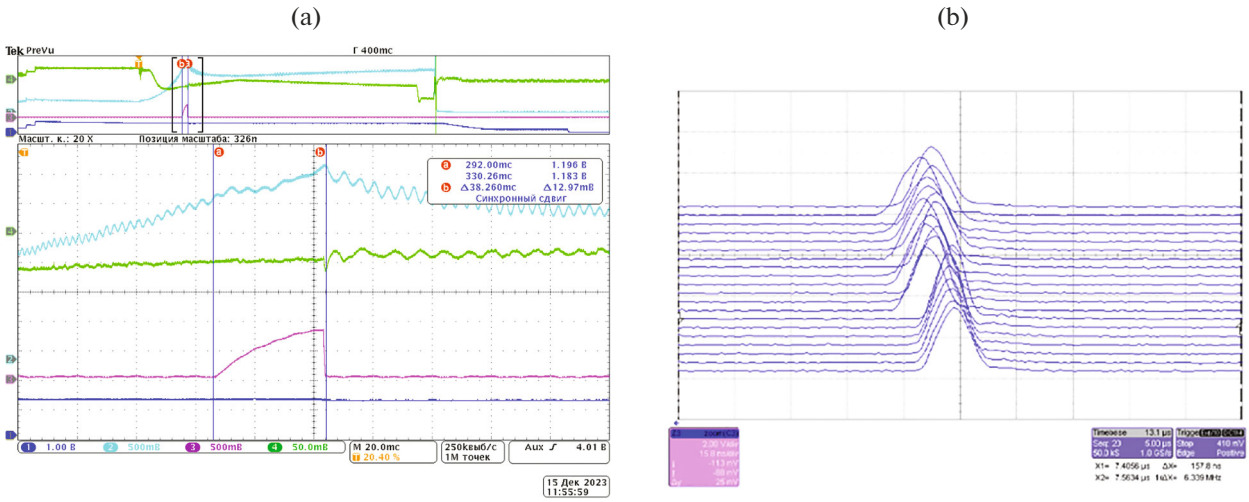

Fig. 6. (a) Transition energy jump in our U-70 session. The green curve shows the signal from the phase sensor; the violet line is the gradient in the windings of the additional quadrupoles; and the blue line is the signal from the peak detector. (b) Longitudinal linear density of the bunch, relative to the RF phase at the moment of the jump.

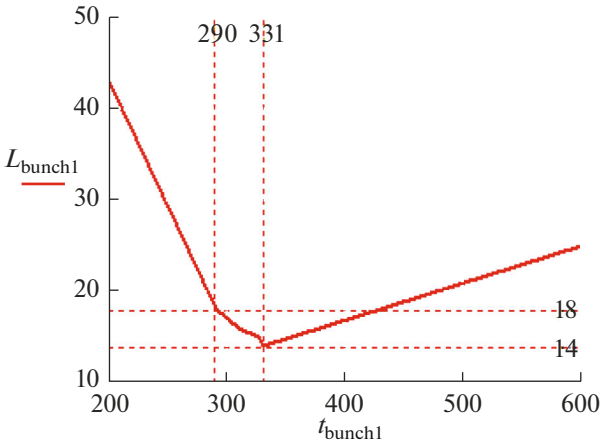

Fig. 7. Change in the bunch length during the acceleration cycle in our U-70 session.

Results from modeling the longitudinal motion (Fig. 8, Table 4) are shown for different models at accelerations of 6.9 to 12.9 GeV [9] for a jump in transition energy and another allowing for impedances of the type $Z_n/n = \pm i \times \text{const}$ and different intensities of acceleration from 6.9 to 8.9 GeV (Fig. 9). The initial values are $\tau_L = 4t_\sigma \simeq 20$ ns at $E_0 = 6.9$ GeV, $\Delta E_0 = 4E_\sigma = 49.3$ MeV, and $\varepsilon_{0.95\%} = 1.16$ eV s.

Comparing the two ways of transition energy crossing (with and without a transition energy jump), we may conclude that the longitudinal length of the bunch was reduced less with a jump. The considered impedances therefore also disturbed the bunch to a lesser extent. An increase in emittance was observed only when considering an intense bunch where the number of particles was $N_{\text{beam}} = 1 \times 10^{12}$ ppb.

CONCLUSIONS

Transition energy crossing in harmonic RF with and without a jump was examined in a session on the U-70 proton synchrotron. The longitudinal dynamics were modeled numerically for different impedances and intensities of bunches. It was shown that the rate

Table 4. The results of numerical simulation of transition energy crossing with jump, taking into account the influence of different impedances for different intensities

Modeling parameters	95% phase volume	Preservation of the beam (9 GeV)	Features
$\alpha_1 = 0$, simple Without impedance	1.165	100%	Simple model Emittance does not increase
$\alpha_1 = 0$, exact Without impedance	1.167	100%	Exact model Emittance does not increase
$\alpha_1 = 0.01$, exact Without impedance	1.174	100%	No nonlinearity Emittance does not increase
$\alpha_1 = 0.01$, exact $Z_n/n = -i10$ 4×10^{11} ppb	1.17	100%	Length shrinks after jump γ_{tr}
$\alpha_1 = 0.01$, exact $Z_n/n = +i10$ 4×10^{11} ppb	1.17	100%	Weak quadrupole oscillations before jump γ_{tr}
$\alpha_1 = 0.01$, exact $Z_n/n = -i10$ 1×10^{12} ppb	1.23	99%	Bunch length shrinks considerably; emittance grows slightly
$\alpha_1 = 0.01$, exact $Z_n/n = +i10$ 1×10^{12} ppb	1.23	99%	High amplitude of quadrupole oscillations; emittance grows slightly

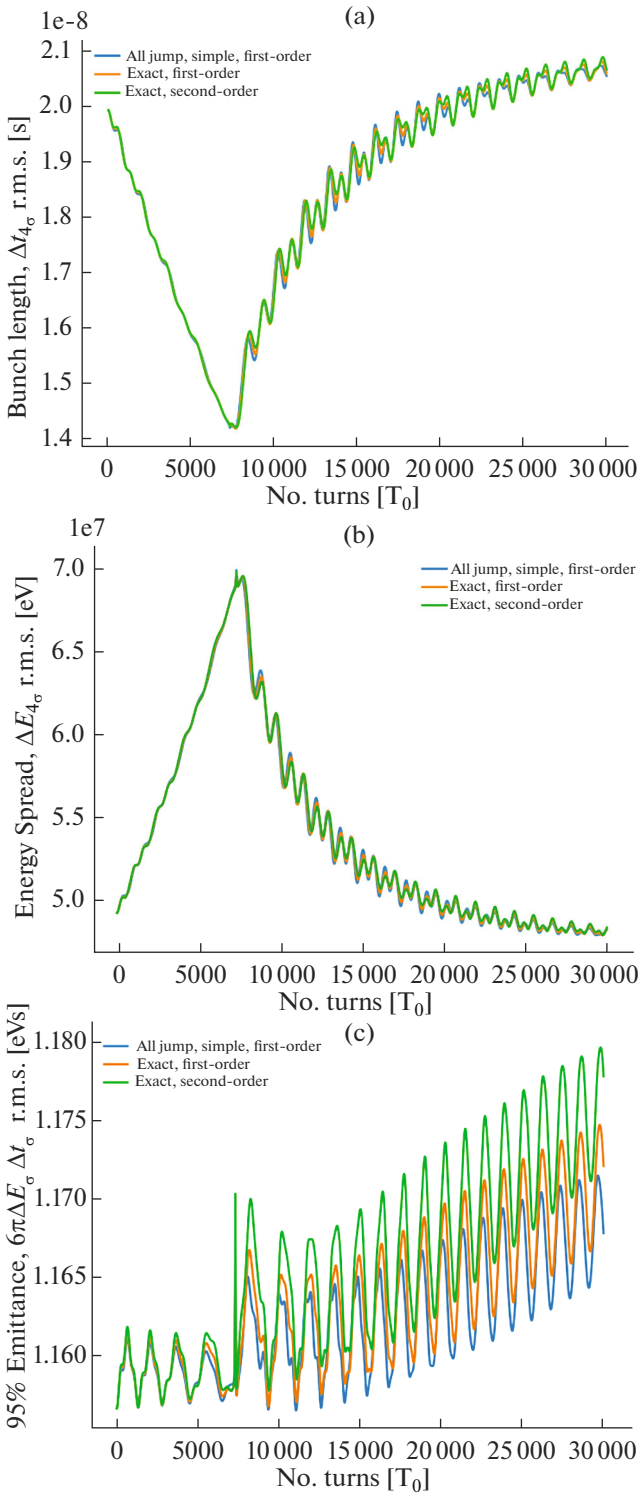

Fig. 8. Dependence of (a) the bunch length, (b) the energy spread inside the bunch, and (c) the longitudinal emittance on the turn number in the vicinity of the transition energy upon changing the energy from 6.9 to 12.9 GeV for three models with a jump, ignoring the impedance. The blue curve considers only the first order $\eta = \eta_0$ for a simple solver; orange, only the $\eta = \eta_0$ for an exact solver; and green, only $\eta = \eta_0 + \eta_1\delta$.

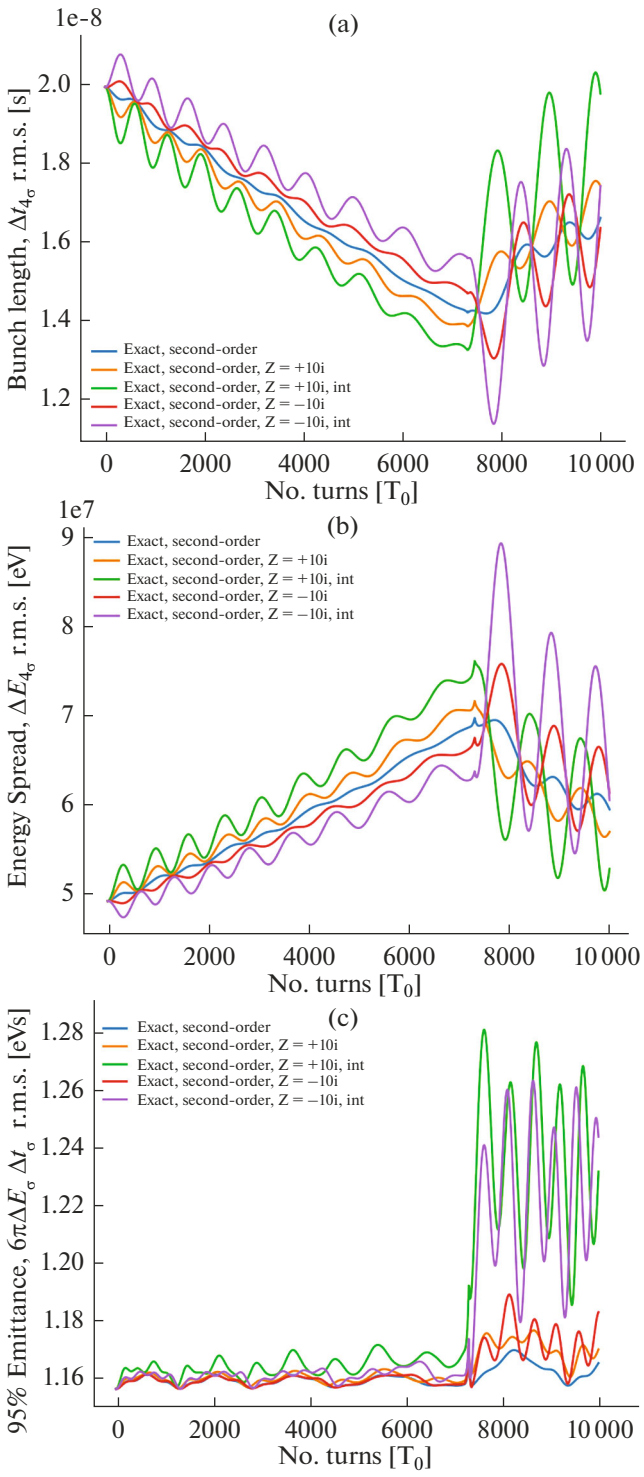

Fig. 9. Dependence of (a) the bunch length, (b) the energy spread inside the bunch, and (c) the longitudinal emittance on the turn number in the vicinity of the transition energy upon changing the energy from 6.9 to 8.9 GeV with a jump, allowing for different types of impedance and intensities.

of acceleration plays a key role in transition energy crossing. A transition energy jump method was used to increase it. The transition energy was changed by modulating the dispersion function, allowing us to control the longitudinal emittance of the bunch at the moment of crossing.

The studied dynamics of longitudinal motion near the transition energy is of interest for further study at the NICA complex.

ACKNOWLEDGMENTS

The authors are grateful to S.V. Ivanov, the director of the Logunov Institute of High Energy Physics (IHEP), for giving us the opportunity to participate in a U-70 synchrotron session; and to IHEP employees V.A. Kalinin, P.T. Pashkov, and A.D. Ermolaev for their comprehensive assistance in our investigation.

FUNDING

This work was supported by ongoing institutional funding. No additional grants to perform or direct this particular research were obtained.

CONFLICT OF INTEREST

The authors of this work declare that they have no conflicts of interest.

REFERENCES

1. W. Hardt, in *Proceedings of the 9th Intenrational Conference on High Energy Acceleration* (Stanford, CA, 1974), p. 434.
2. J. Wei, in *Proceedings of the EPAC92* (1992), Vol. 1, p. 643.
3. P. T. Pashkov, Measuring inductive component of longitudinal coupling impedance in IHEP PS using γ-transition jump, Preprint No. 2004-4, IVFE (Institute for High Energy Physics, Protvino, Moscow oblast, 2004).
4. S. Y. Lee, *Accelerator Physics*, 4th ed. (World Scientific, Singapore, 2018). https://doi.org/10.1142/11111
5. K. Y. Ng, in *Proceedings of the US Particle Accelerator School (USPAS 2002)* (FermiLab, 2002).
6. MADX. https://mad.web.cern.ch/mad/.
7. BLonD. https://blond.web.cern.ch/.
8. P. T. Pashkov, *Fundamentals of Proton Synchrotron Theory: A Textbook for Students of the Lomonosov Moscow State University* (Institut Fiziki Vysokikh Energii, Protvino, Moscow oblast, 1999).
9. S. A. Chernyi, Fiz. Elem. Chastits At. Yadra **22**, 1067 (1991).
10. V. Lebedev, OptiM code. Private communication. www.bdnew.fnal.gov/pba/organizationalchart/lebedev/OptiM/optim.htm.